Journal of Biomolecular NMR, 2 (1992) 407–420
ESCOM

J-Bio NMR 073

Solution conformation of human big endothelin-1*

Mary L. Donlan, Frank K. Brown and Peter W. Jeffs**

Glaxo Research Institute, 5 Moore Drive, Research Triangle Park, NC 27709, U.S.A.

Received 13 April 1992
Accepted 9 June 1992

Keywords: Big endothelin structure; Solution structure by NMR

SUMMARY

The solution conformation of human big endothelin-1, a 38-residue peptide which serves as the putative precursor to the potent vasoconstrictor endothelin-1 has been examined by ^{1}H NMR. NOEs were utilized as distance restraints in the distance geometry program DSPACE to generate initial structures. Further refinement of these structures was accomplished through molecular mechanics/molecular dynamics in an iterative process involving the incorporation of stereospecific assignments of prochiral centers and the use of back-calculation of NOESY spectra. A family of structures consisting of a type II β-turn for residues 5-8 and an α-helix extending from residues 9–16 constitute a well-defined region, as reflected by the atomic root-mean-square (RMS) difference of 1.56 Å about the mean coordinate positions of the backbone atoms (N, C, Cα and O). This core region (residues 1–15) is very similar to the core residues of endothelin-1 (Donlan, M. et al. (1991) *J. Cell. Biochemistry*, **S15G**, 85). While the evidence from NOESY and coupling constant data suggests that the C-terminal region, residues 17–34, is not a mixture of randomly distributed chain conformations, it is also not consistent with a single chain conformation. Under the conditions studied, residues 17–38 in human big endothelin-1 in water at pH 3.0 between 20–30°C appear to be represented by a series of conformers in dynamic equilibrium.

INTRODUCTION

Endothelin-1 (ET-1) and related peptides ET-2, ET-3, ET-β and the structurally homologous snake venom sarafotoxins (Inoue et al., 1989; Kloog and Sokolovsky, 1989; Saida et al., 1989) produce a variety of pharmacological effects in both vascular and nonvascular tissue (Yanagisawa and Masaki, 1989; Simonson and Dunn, 1991). The biosynthetic pathway to endothelin-1, a 21-residue peptide, involves a 38-amino acid precursor peptide referred to as big endothelin (Yanagisawa et al., 1988). As outlined in Fig. 1, the pathway to endothelin is proposed to involve the

* *Supplementary material available from the corresponding author*: Appendix I (final list of NOE restraints, 6 pages) and Appendix II ($^3J_{NH/\alpha H}$ scalar couplings, 1 page) used for structure calculations are available as supplementary material. Appendix III, table of structural statistics showing: (a) deviations from idealized geometry with energies greater than 1.2 kcal/mol; and (b) evaluation of nonbonded contacts. Ordering information is given on any masthead.

** To whom correspondence should be addressed.

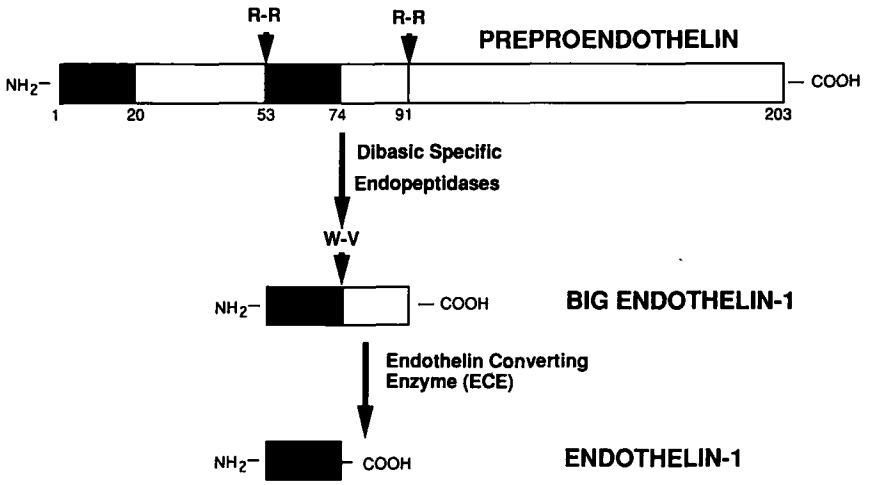

Fig. 1. The proposed biosynthetic pathway for the proteolytic processing of preproendothelin (203 amino acids) to endothelin-1 (21 amino acids) (Yanagisawa et al., 1988).

proteolytic processing of a 203-amino acid preproendothelin. Through initial processing by carboxypeptidases and endopeptidases at dibasic amino acid sites, the 38 (human)- or 39 (porcine)-amino acid intermediate species referred to as 'big endothelin-1' is formed. Big endothelin-1 is further processed enzymatically at an unusual proteolytic cleavage site between residues Trp^{22} and Val^{23} by an endothelin-converting enzyme (ECE) to form ET-1. The presence of both big ET-1 and the carboxyl-terminal fragment of big ET-1 (residues 22–38/39) in conditioned endothelial medium supports this biosynthetic pathway (Emori et al., 1989; Sawamura et al., 1989).

The discovery of pharmacological agents that block the generation of endothelin from its essentially inactive precursor big endothelin or antagonize its binding to cellular receptors is of considerable interest as a means of assessing the physiological role of endothelin. We have undertaken structural studies of endothelin (Donlan et al., in preparation) and big endothelin as a means of gaining insight into structural factors important in ET receptor binding. Elucidation of the solution structure of big endothelin, which is the subject of this report, is also of potential interest in providing an understanding of the unusual specificity of ECE. After considerable effort, the physiologically relevant enzyme involved in the conversion of big ET-1 to ET-1 has been identified as a phosphoramidon-sensitive neutral metalloproteinase (Matsumura et al., 1990; Nichols et al., 1990; Ohnaka et al., 1990), which is an enzyme other than neutral endopeptidase EC 3.4.24.11 (NEP 24.11) (Ikegawa et al., 1990; Pollack and Opgenorth, 1991).

In this paper, we report the detailed analysis of ^1H NMR studies carried out in aqueous solution, and the derivation of the 3D structure of human big ET-1 accomplished via an iterative procedure of distance geometry, molecular dynamics, and NOESY back-calculation.

EXPERIMENTAL PROCEDURES

NMR spectroscopy

Big endothelin-1 (human), obtained from Peptides International, was dissolved to a concentration of 0.5 mM, pH 3.0, in 50 mM sodium acetate-d_3 (95% H_2O/5% D_2O).

Two-dimensional NMR spectra were obtained for big ET-1 in either H_2O or D_2O at 20°C and 30°C with a Bruker AMX600 spectrometer. Typically, spectra were collected with 2K complex data points over a sweep width of 8 kHz. All spectra were collected in the phase-sensitive mode and, except when noted below, TPPI phase cycling was used.

Nuclear Overhauser enhancement (NOESY) spectra (Jeener et al., 1979) were obtained for H_2O and D_2O solutions at mixing times of 100, 200, 300 and 400 ms. Spectra were collected with 512 points in t_1 and 2048 complex points in t_2 with 64 scans per t_1 value. For NOESY spectra obtained in H_2O, solvent suppression was accomplished using a 1-1 jump-return pulse. For all other experiments, presaturation was used for solvent suppression. Double-quantum-filtered correlated spectroscopy (DQF-COSY) experiments (Rance et al., 1983) were undertaken on solutions in H_2O and D_2O with 1024 t_1 points and 2048 complex points in t_2 with 96 scans per t_1 value. Homonuclear Hartmann–Hahn (HOHAHA) spectra (Braunschweiler and Ernst, 1983) were collected with mixing times of 45, 65 and 75 ms, using an MLEV-17 sequence for isotropic mixing (Bax and Davis, 1985). Experimental conditions for HOHAHA experiments were similar to those described for NOESY spectra. In order to obtain stereospecific assignments, a P.E.-COSY experiment (Mueller, 1987) was performed in D_2O using hypercomplex phase cycling. In this experiment, 4096 points were collected in t_2 for 1024 t_1 values (64 scans per t_1 value). NMR processing and cross-peak volume integration were performed on a Silicon Graphics Personal Iris using the software package FELIX 1.1 (Hare Research, Inc.). All structure calculations and refinements were carried out on an Iris SG380/4D computer.

An iterative method of structure calculation was utilized to elucidate the 3D structure of big ET-1 in aqueous solution. This general procedure consists of a repetitive cycle which begins with initial generation of structures by distance geometry (DSPACE, Hare Research, Inc.), followed by molecular mechanics/molecular dynamics refinement (AMBER 3.0) (Singh et al., 1986; Weiner et al., 1984) and the resulting structures are subjected to a NOESY back-calculation (BKCALC, Hare Research, Inc.).

Initial structures were obtained from the NOE data via distance geometry calculations in which the metric matrix program DSPACE (Hare Research, Inc.) was utilized. Using the experimentally derived distances and distances implicit in the primary sequence of the peptide, i.e. covalent bond lengths and bond angles, a bounds matrix was prepared which was subsequently smoothed using triangle and inverse triangle inequalities (Crippen, 1981; Havel et al., 1983). This matrix was embedded in 3D space (Crippen, 1977) and the resulting structures were refined to minimize the 'penalty' function. This 'penalty' function is a measurement of the deviation between distances/information in the structure and the bounds matrix. Refinement was accomplished using repetitive cycles of conjugate gradient minimization and simulated annealing (Nerdal et al., 1988; Kraulis et al., 1989). The generation of structures using this approach has previously been described (Summers et al., 1990). The final set of NOE constraints can be obtained as supplementary material (Appendix I).

The initial structures obtained from distance geometry were further refined using a min-md-min refinement approach with AMBER 3.0 (Singh et al., 1986), in which the experimentally derived interproton distances were added as an additional energy term. Both minimizations and molecular dynamics simulations were carried out using a distance-dependent dielectric constant equal to 80 with a nonbond update every 50 steps. A square well harmonic restraint was used for the NOE distances. The refinement procedure employed involved a sequence of steps as follows: (1) struc-

tures were minimized using 100 steps of steepest descent and 2400 steps of conjugate gradient refinement with a force constant for the NOE penalty function of 50 kcal/molÅ^2; (2) these structures were subjected to 10 ps of dynamics with heating to 300 K (force constant = 50 kcal/molÅ^2); (3) structures were subjected to minimization using 100 steps of steepest descent and 2400 steps of conjugate gradient refinement (force constant = 50 kcal/molÅ^2); and (4) reminimization of the previous set of structures was performed using 50 steps of steepest descent and 450 steps of conjugate gradient refinement with the force constant for the NOE penalty function equal to 5 kcal/molÅ^2. This last step of minimization was undertaken to ensure that the force constant of 50 kcal/molÅ^2 did not highly distort the resulting structures. As a control, the NOE restraints were eliminated after the last step of refinement and the total energies of the structures were compared. This allowed for the assessment of strain energy introduced by the NOE restraints. The AMBER refinement protocol was followed by a comprehensive analysis of the bonds, angles and torsional energies.

After the AMBER simulations, refinement of the resulting structures was accomplished by back-calculation of the NOESY spectra using BKCALC (Hare Research, Inc.). As previously described (Nerdal et al., 1989; Summers et al., 1990), this procedure involves a numerical integration of the Bloch equations and the simulated NOESY data is compared with the experimental data. In the case of back-calculation of big endothelin NOESY spectra, the back-calculation procedure was used as a qualitative rather than a quantitative measurement. This aided structure refinement by providing additional restraints for those protons that gave rise to a minor cross peak or cross peaks that were difficult to identify due to spectral overlap. In addition, it provided non-NOE restraints in which the lower bound was set to 5.00 Å when the absence of a cross peak was experimentally verified. These additional restraints were added to the initial list of distances and used in further structure refinement. In addition, after several iterations some of the experimental bounds were narrowed, based on the agreement between the experimental and simulated NOEs.

At the start of initial distance geometry calculations, stereospecific assignments had not been performed. Thus the diastereotopic methylene protons and methyl groups were designated as nonchiral, which allowed the protons to float between *pro*-R and *pro*-S in DSPACE calculations (Weber et al., 1988). At a later stage of refinement, stereospecific assignments of many of these resonances were accomplished using measurements of the $^3J_{H\alpha,H\beta}$ coupling constants obtained in the P.E.-COSY experiment in conjunction with the NOESY data (Hyberts et al., 1987). For several other residues, specifically residues L6, V12, and D18, the stereospecific assignments were obtained as a result of the structure calculations. These stereospecific assignments were also used in further structure refinement.

This iterative procedure of distance geometry, min-md-min, and NOESY back-calculation was repeated for several iterations until satisfactory agreement was obtained between the experimental data and final structures. Satisfactory agreement was judged as a small number of NOE violations in the final structures and qualitative agreement of the cross peaks seen in the experimental and simulated NOESY spectra.

NMR restraint analysis was carried out on the NOE data using an algorithm initially described by Hempel (1989) and Brown et al. (1992). This analysis provides information regarding the correlation of NOE data with defined structures. Specifically, three levels of correlation are defined: (1) highly correlated regions which occur within clusters or domains, (2) weakly correlated regions which are made up of pendant templates to domains, and (3) uncorrelated regions in which there are no shared NOEs with other regions/domains.

TABLE I
^{1}H CHEMICAL-SHIFT ASSIGNMENTS OF BIG ET-1 AT pH 3.0 AND 20°C, 50 mM SODIUM 1-ACETATE

Residue	NH	$C^{\alpha}H$	$C^{\beta}H$ (r)	$C^{\beta}H$ (s)	Other
Cys^{1}		4.31	3.25	3.25	
Ser^{2}	8.92	4.67	3.77	3.77	
Cys^{3}	8.29	4.94	2.48[a]	3.13[a]	
Ser^{4}	8.94	4.25	3.90	3.85	
Ser^{5}	7.80	4.52	3.88	3.69	
Leu^{6}	8.53	4.11	1.58[a]	1.52[a]	γH 1.58 δCH_3 0.74, 0.82
Met^{7}	7.97	4.38	2.13[a]	1.83[a]	γCH_2 2.41, 2.58 εCH_3 2.12
Asp^{8}	7.37	4.63	3.11[a]	2.68[a]	
Lys^{9}	8.18	3.82	1.75	1.75	γCH_2 1.33, 1.43 δH_2 1.58, 1.58 εCH_2 2.88, 2.88 εNH_3^+ 7.53
Glu^{10}	8.37	4.15	2.06	2.06	γCH_2 2.41, 2.41
Cys^{11}	7.60	4.24	3.06[a]	3.13[a]	
Val^{12}	8.11	3.45	1.97		γCH_3 0.79[a], 0.92[a]
Tyr^{13}	7.78	4.25	2.96	2.96	2,6H 6.84 3,5H 6.67
Phe^{14}	8.23	4.12	3.15	3.15	2,6H 7.33 3,5H 7.26 4H 7.26
Cys^{15}	8.53	4.53	2.87	3.20	
His^{16}	7.87	4.42	3.24	3.24	2H 8.41 4H 7.11
Leu^{17}	7.88	4.20	1.54[a]	1.45[a]	γH 1.48 δCH_3 0.74, 0.74
Asp^{18}	8.31	4.51	2.65[a]	2.76[a]	
Ile^{19}	7.75	4.03	1.65		γCH_2 0.99, 1.30 γCH_3 0.55 δCH_3 0.73
Ile^{20}	7.97	4.03	1.70		γCH_2 1.03, 1.30 γCH_3 0.71 δCH_3 0.71
Trp^{21}	8.15	4.60	3.17	3.08	2H 7.18 4H 7.49 5H 7.01 6H 7.09 7H 7.35 NH 9.99
Val^{22}	7.80	3.93	1.88		γCH_3 0.77, 0.77
Asn^{23}	8.27	4.60	2.72	2.58	γNH_2 8.05, 8.05
Thr^{24}	8.05	4.54	4.10		γCH_3 1.14
Pro^{25}		4.30	2.19	2.19	γCH_2 1.77, 1.88 δCH_2 3.62, 3.72
Glu^{26}	8.27	4.28	1.84	1.84	CH_2 2.30, 2.30
His^{27}	8.37	4.64	3.15	3.07	2H 8.48 4H 7.17
Val^{28}	8.16	4.07	1.92		γCH_3 0.82, 0.82
Val^{29}	8.26	4.15	1.93		γCH_3 0.81, 0.81
Pro^{30}		4.29	2.14	2.14	γCH_2 1.76, 1.88 δCH_2 3.55, 3.77
Tyr^{31}	8.06	4.41	2.93	2.93	2,6H 7.03 3,5H 6.75
Gly^{32}	8.18	3.79, 3.74			
Leu^{33}	8.00	4.26	1.54	1.54	γH 1.52 δCH_3 0.79, 0.84
Gly^{34}	8.40	3.87, 3.85			
Ser^{35}	8.06		3.80	3.72	
Pro^{36}		4.37	2.01	2.01	γCH_2 1.88, 1.95 δCH_2 3.62, 3.72
Arg^{37}	8.39	4.29	1.82	1.68	γCH_2 1.58, 1.58 δCH_2 3.11, 3.11 NH 7.12
Ser^{38}	8.04	4.27	3.82	3.77	

[a]Indicates stereospecific assignments

RESULTS AND DISCUSSION

Assignments of the proton resonances for big endothelin-1 in aqueous solution were obtained using the standard sequential assignment strategy (Wüthrich et al., 1986). Analysis of spectra obtained at 20°C and 30°C was undertaken to provide unambiguous assignment of all the proton chemical shifts. A summary of the chemical shifts for human big ET-1 at pH 3.0 and 20°C is given in Table 1. Figure 2 shows the observed amide-alpha sequential connectivities observed in the NOESY spectrum (mixing time = 400 ms) of big ET-1. It was possible to trace all of the Hα-NH sequential connectivities (except for connectivities involving proline residues) through residue Ser^{35}. However, the carboxyl-terminal residues Arg^{37} and Ser^{38} did not show any NOESY cross peaks even at 20°C, indicating these residues are undergoing very fast motion on the NMR time scale. Despite the lack of NOEs corresponding to these residues, the expected scalarly coupled cross peaks were observed in the DQF-COSY, thereby permitting their unambiguous assignment.

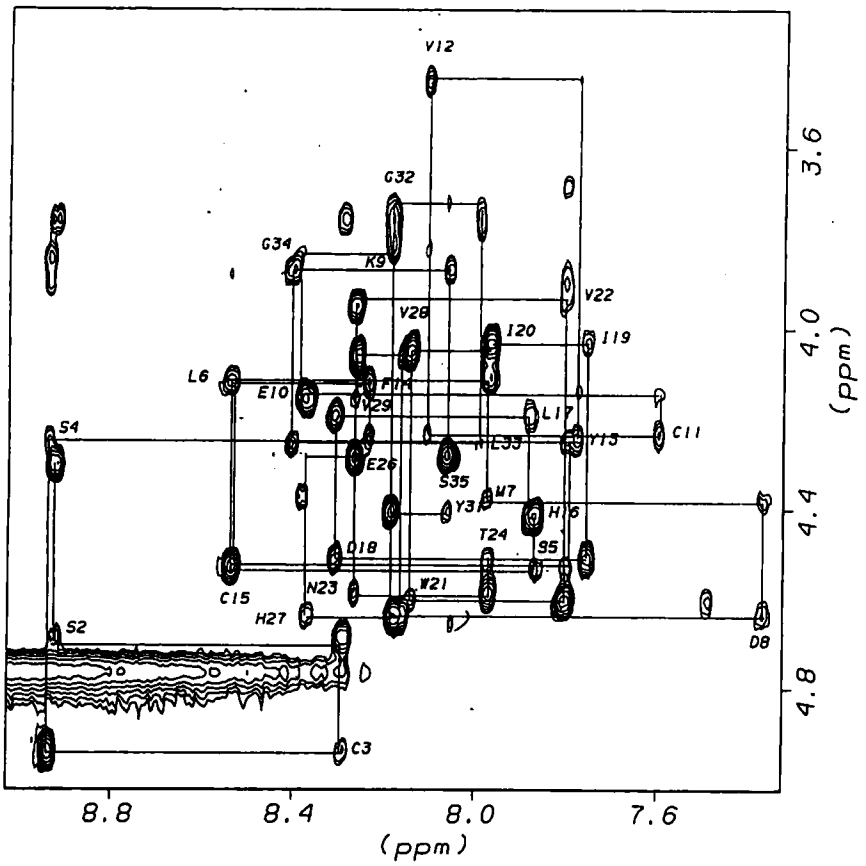

Fig. 2. Finger-print region of the NOESY spectrum of big endothelin-1 showing the sequential amide-alpha proton connectivities. The spectrum was acquired on a Bruker AMX600 with a mixing time of 400 ms in 50 mM sodium acetate-d_3, pH 3.0 at 20°C.

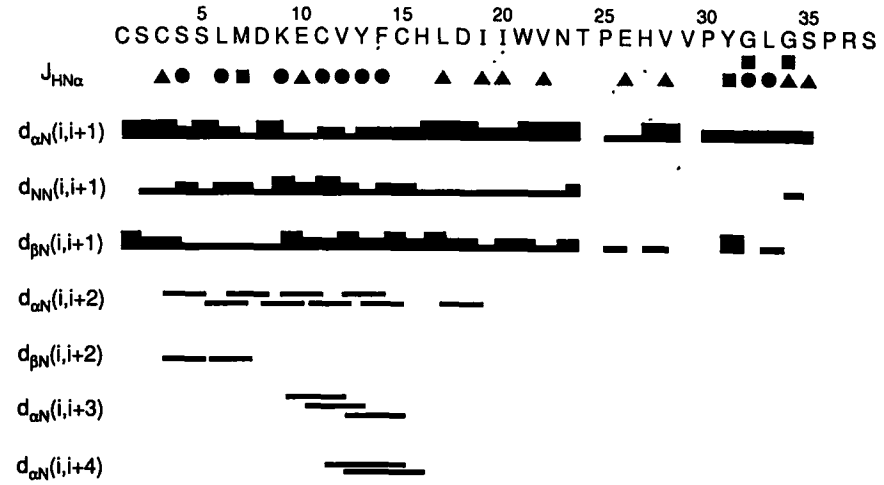

Fig. 3. Amino acid sequence of big ET-1 with a summary of the sequential assignments and coupling constants. The intensities of the NOEs are indicated by the thickness of the blocks. Long-range NOEs are also indicated. $^3J_{NH\alpha}$ coupling constants are indicated as follows: ▲ > 7 Hz, ● < 7 Hz and ■ ≈ 7 Hz.

In order to observe the NOE build-up rates, NOESY spectra were collected with mixing times over a range of 100–400 ms. Figure 3 shows a summary of the observed NOEs including both sequential and long-range interactions. In addition, the $^3J_{NH/\alpha H}$ scalar couplings which were measured from P.E.-COSY experiments are presented. The $^3J_{NH/\alpha H}$ scalar couplings are available as supplementary information (Appendix II). A qualitative analysis of the NOE and coupling-constant data indicates residues 5–8 are in a type II β-turn structure, residues 9–16/17 form a stable α-helix, and another β-turn region exists around residue 33..

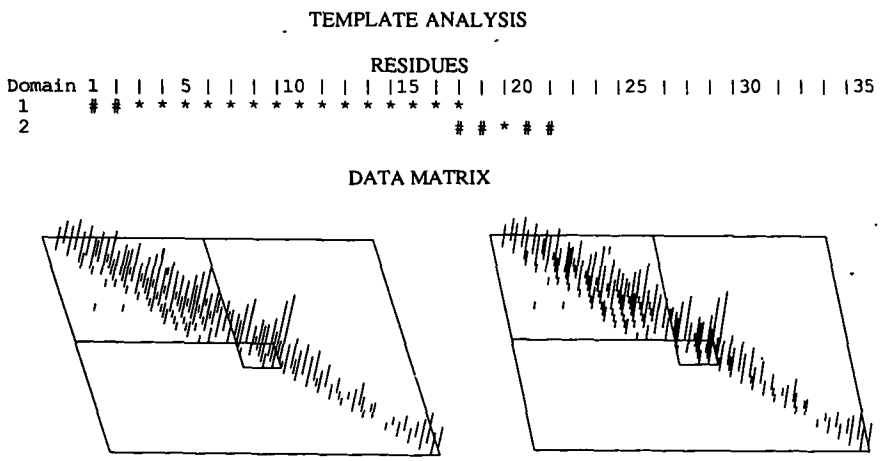

Fig. 4. The NMR restraint analysis would indicate a well-defined structure for residues 3–17, and residues 17–21 would have pendant interactions. The * represents correlated data. A # represents pendant data, and a blank corresponds to the lack of conformationally restrictive data. Below the template analysis is a stereoview of the data matrix. The large box highlights residues 1–17, and the small box highlights residues 17–22. The length of the line is proportional to the number of NOEs corresponding to the residues.

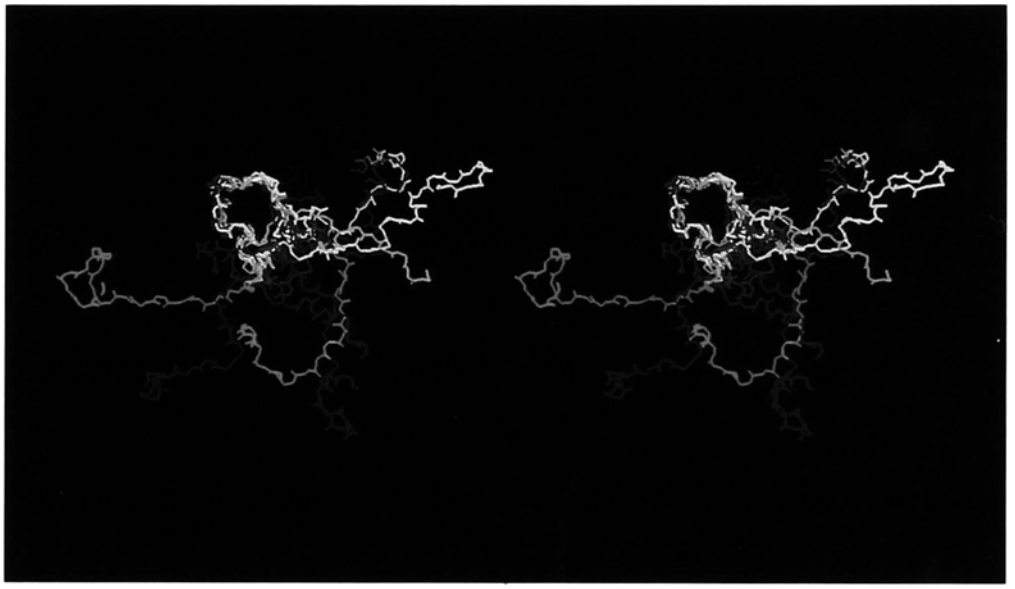

Fig. 5. (A) Stereoview of the superimposition of the backbone atoms (N, C, Cα and O) of residues 1–15 in a set of representative structures of big endothelin-1. The average RMSD of this set of structures for backbone residues 1–15 is 1.56 Å.

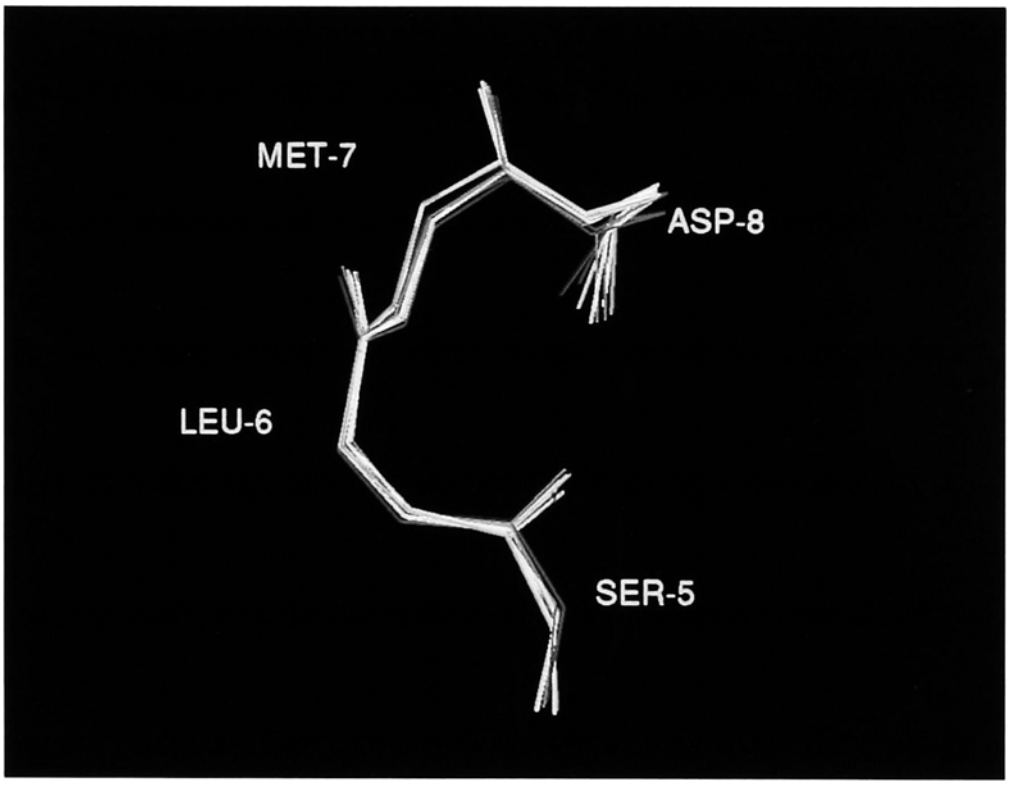

Fig. 5. (B) View of the superimposition of the backbone atoms (N, C, Cα and O) of the β-turn region involving residues 5–8 of big endothelin-1. The average RMSD of this set of structures for residues 5–8 is 0.41 Å.

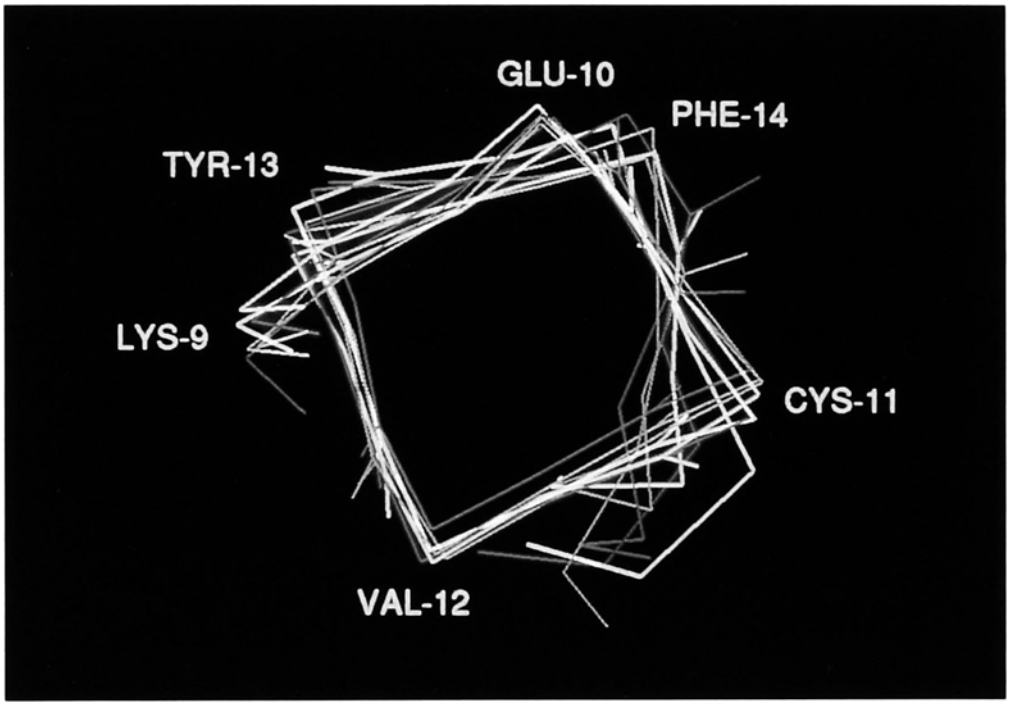

Fig. 5. (C) View of the superimposition of the backbone atoms (N, C, Cα and O) of the helix (residues 9–15) of big endothelin-1. The average RMSD of this set of structures for residues 9–15 is 0.84 Å.

NOE cross peaks were initially converted to distance bounds by classifying the NOE intensity as strong, medium or weak with upper distance restraints of 2.5, 3.5, or 4.5 Å, respectively. The lower bound was assigned to 1.8 Å. An initial set of 473 NOEs consisting of 253 intraresidue and 220 interresidue NOEs was extracted from the NOESY spectra. No hydrogen bond or disulfide bond distances were included as restraints in the refinement process.

As previously described, an iterative procedure of structure determination was carried out to elucidate the 3D structure of big ET-1. This procedure involved a cycle of distance geometry, molecular mechanics/molecular dynamics, and NOESY back-calculation.

The structure calculations indicate that residues 5–8 are in a type II β-turn structure, residues 9–15 form an α-helix while the remaining residues of big ET-1 show conformational averaging and do not have any well-defined structure. Residues 36–38 were omitted from all structural/NOE analyses since the NOESY data suggest these are extremely mobile residues. These results are in general agreement with the qualitative observations made from the NOE and coupling-constant data, except for the second β-turn, which was proposed from the qualitative analysis of the NOE and coupling-constant data to exist around residue 33. This residue is close to the C-terminus, which is undergoing rapid motions, and there are not enough unambiguous distances in this region to define this proposed β-turn. In addition, it should be noted that although residues 17–35 were conformationally averaged, the prolines at positions 25 and 30 did not adopt a cis X-Pro peptide bond in the calculated structures. This is consistent with the experimental NOESY data in which NOEs were seen between αH_i and $\delta CH_{2(i+1)}$ of X-Pro residues while NOEs between αH_i and αH_{i+1} were absent.

An NMR restraint analysis routine (Hempel, 1989; Brown et al., 1992) was applied to the NOE distance restraints. The results from this analysis as shown in Fig. 4 indicate that NOEs associated with residues 3–17 are very well correlated (upper and lower bounds defining a fixed 3D structural unit), while residues 1–3, and 17–21 show pendant interactions (upper and lower bounds which define a 2D structural unit), and residues 22–35 are uncorrelated. These data suggested that although there are some regions of big ET-1 which are conformationally undefined, there are large regions of the molecule which appear to be highly structured. Specifically, there is a stretch in the sequence between residues 3 and 17 which should form a well-defined structure; residues 17–21 should also have some structure and residues 22–35 are unconstrained and therefore expected to have an uncorrelated structure.

The results of the structure calculations do not fully agree with the results obtained from the NMR restraint analysis of the NOE restraints. In agreement with the NMR restraint analysis, residues 3–16 possess a very well defined structure; however, residues 17–21/22 have an averaged structure. The NMR restraint analysis suggested that residues 17–21/22 have some type of regular structure e.g. secondary structural elements. The discrepancy between the NMR restraint analysis and the final structures can be attributed to several factors. Two possible explanations are: (1) the restraint analysis does not work adequately for short stretches, 3–4 Å, in a peptide structure, or (2) the data are not self-consistent. In this study, the latter explanation is believed to be the main factor, since the data in the region 17–22 cannot all be simultaneously satisfied. Thus, the data are reduced to the restraints which are satisfied. Since the data are pendant in the region 17–21/22, reduction of the data by any amount would abolish the weak correlation, leading to an uncorrelated region.

It is probable that the discrepancies observed result from conformational averaging. Average structures can give the appearance of more accurate data than actually exist; i.e., in one conformation the molecule has A and B close while in another conformation, C and D are close, with the criterion that if A and B are near each other C and D cannot be close and vice versa. Under these circumstances, two NOEs may appear, while for each structure only one NOE can exist at a time. This would effectively reduce the information by one half. The data reduction could render a pendant region to an uncorrelated region. Thus, the NMR restraint analysis helped us to highlight a region of difficulty, in which a discrepancy between the predicted and experimental results can be rationalized due to the lack of self-consistency produced by conformationally averaged data.

The final structures were evaluated by several methods. The Ramachandran maps were plotted and any structures which had more than 4–5 residues with disallowed phi–psi angles were discarded. In addition, back-calculation of the NOESY spectra was used as a criterion for evaluation of the structures, i.e. satisfactory agreement of the calculated and experimental data was essential. The final family of 11 structures did not contain any structures which had more than 1–2 NOE violations greater than 0.4 Å. For the calculation of the number of NOE violations, only those residues that were conformationally restrained were used to evaluate these final structures. In addition, the structures were analyzed for strain energy and van der Waals (VDW) contacts. The results indicated that 5 of the 11 structures did not have a strain energy greater than 1.2 kcal/mol, while the other structures showed only angle strain energy with a maximum of two angles greater than 1.2 kcal/mol. In most cases the strain energy was associated with the Cα-N-Cδ angle of Pro^{25}. An evaluation of the VDW contacts demonstrated that there were no bad interactions and that VDW energies for all of the structures were negative. (See Appendix III in supplementary material.)

Figure 5A shows a stereoview of the superimposition of 11 representative structures in which the backbone atoms (N, C, Cα and O) of residues 1–15 are superimposed. The average RMS deviation of the backbone atoms of residues 1–15 of these 11 structures is 1.56 Å. Figures 5B and 5C show views of the superimpositions of the two major elements of secondary structure. The average RMS deviation of the backbone atoms of the β-turn region (residues 5–8) is 0.41 Å (Fig. 5B) while the average RMS deviation for the α-helix (residues 9–15) is 0.84. The RMS deviation of the calculated structures about the mean coordinates is 0.98 for the backbone atoms and 1.38 for all atoms of residues 1–15. The RMS deviation of the 11 individual structures used in this calculation from the average structure for the backbone atoms and all atoms is shown in Table 2.

Both big ET-1 and ET-1 contain the same basic elements of secondary structure – a type II β-turn from residues 5–8, a right-handed α-helix from residues 9–15/16, and a conformationally averaged structure after residue 17 (Munro et al., 1991; Reilly and Dunbar, 1991; Donlan et al., in preparation). The core regions (residues 1–15) of both peptides are very similar. Figure 6 shows a comparison of residues 1–21 of big ET-1 and ET-1. Although the global structure appears to be very similar, some subtle differences between the two structures exist. The β-turn region of big ET-1 seems to be slightly more structured than in ET-1. The average RMS deviation of the β-turn region (residues 5–8, backbone atoms) of ET-1 is 1.46 Å as compared to 0.41 for big ET-1, while the helices of both molecules are similar. The average RMS deviation for the α-helix residues 9–15 in ET-1 is 0.65 and 0.84 in big ET-1. The number of NOEs in each of these regions is similar in ET-1 and big ET-1. The significance of these differences in the bicyclic core region of ET-1 and big ET-1 in relation to the large differences in affinity ($> 1.6 \times 10^3$-fold) which they exhibit for the ET indicate the importance of the bicyclic core region for receptor binding, but unless Trp^{21} is present in addition to the requisite core region, no functional vasoconstrictor activity is observed (Kimura et al., 1988; Watanabe et al., 1991).

The results from structure calculations indicate that the residues near the cleavage site of ECE

TABLE 2
RMSD (Å) FROM THE AVERAGE STRUCTURE[a] OF THE FAMILY OF STRUCTURES USED IN THE STRUCTURE ANALYSIS OF BIG ENDOTHELIN-1[b]

Structure	Backbone	All
1	0.89	1.34
2	1.05	1.73
3	1.15	1.79
4	1.28	1.92
5	1.14	1.79
6	1.05	1.71
7	2.12	2.50
8	0.83	1.21
9	1.01	1.38
10	0.91	1.52
11	1.43	2.26

[a] The data presented are for residues 1–15.

[b] Among these structures, there were none that had more than 1–2 NOE violations greater than 0.4 Å. In addition, the van der Waals energies of these structures were all negative and contained no bad contacts.

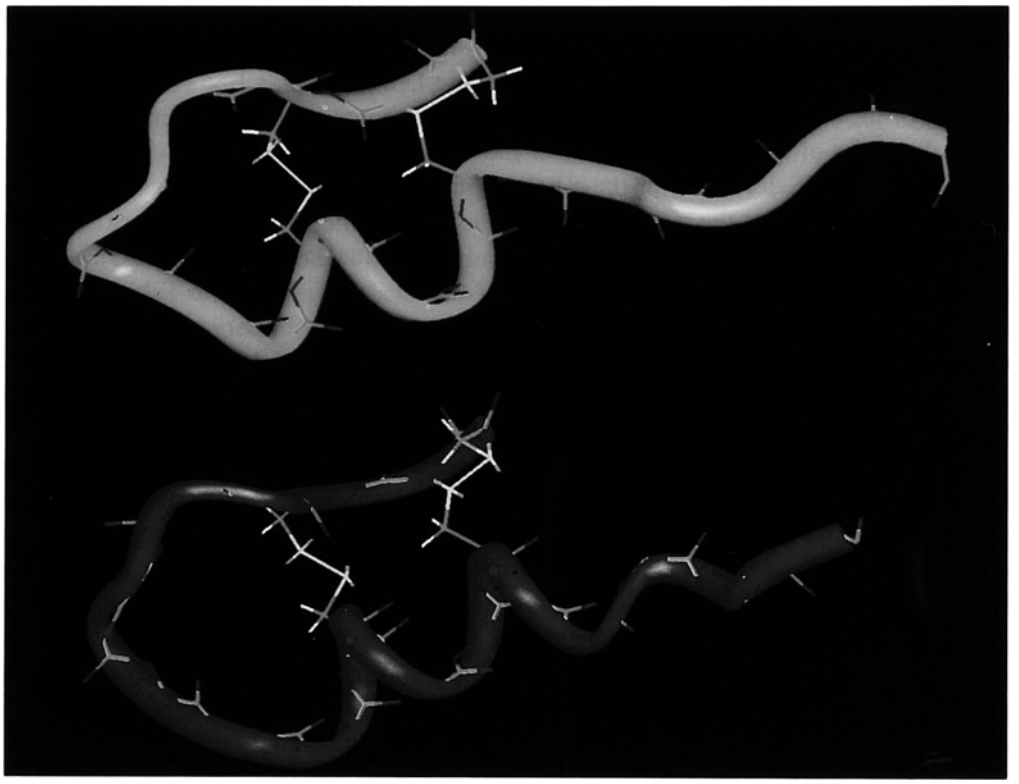

Fig. 6. View of tubular drawings of representative structures of endothelin-1 (top) and that of the first 21 residues of big endothelin-1 (bottom). The structural similarities in the core region (residues 1–15) are apparent as are the minor differences.

are conformationally averaged and have a larger degree of flexibility than the core region of the molecule. This conformational flexibility may allow the peptide to bind the ECE more easily than would be the case if this region was locked into one conformation.

Since there are few X-ray or NMR structures available for prohormones, several theories have been proposed regarding the structural aspects of the proteolytic processing of prohormones. These hypotheses suggest that a common secondary structural feature such as an Ω loop (Bek and Berry, 1990) or a β-turn (Rholam et al., 1986; Brakch et al., 1989) is located at or near the proteolytic cleavage site and is recognized by the converting enzyme. It was suggested that this common structural feature was part of a general coding system for endoproteases involved in prohormone processing (Brakch et al., 1989). In general, these models apply secondary structure prediction methods to primary sequences of peptide prohormones. In most cases, a dibasic doublet comprised of arginine and lysine residues was at the proteolytic processing site in these analyses. When Chou–Fasman methods were used to predict the secondary structure of big ET-1, the analysis also suggested that there is a high probability that a β-turn could exist near the enzyme cleavage site. Obviously, the experimental results in this study do not support this prediction.

In aqueous solution, big ET-1 does not adopt this proposed structure. In fact, the final big ET-1 structures lack tertiary structure, which presumably would be very important in the functional

role of this molecule. It is not unprecedented for hormones to demonstrate conformational changes when in association with a receptor or processing enzyme, and the suggestion that this prohormone exists in another structure when associated with ECE is further substantiated by structure–activity relationships which indicate that the C-terminal region of big ET-1 has a high binding affinity for ECE (Okada et al., 1991). In the structures presented here, this region of big ET-1 was completely flexible, thus it was evident there is no single conformation for this region of the molecule in the free, unbound state. NMR studies carried out on atrial natriuretic factor (ANF) in water and dimethyl sulfoxide-d6 (Fesik et al., 1987; Theriault et al., 1987) indicated that ANF did not adopt any preferred conformation while studies of ANF in sodium dodecyl sulfate micelles indicated that the hormone was structured (Olejniczak et al., 1988).

CONCLUSION

Structures of big ET-1 in aqueous solution have been derived using an iterative procedure of distance geometry, min-md-min and NOESY back calculation. The resulting structures satisfy the experimental restraints for regions of the structures which are well defined. The core region (residues 1–15) adopts a structure similar not only to endothelin-1 (Donlan et al., 1991; Krystek et al., 1991), but also to endothelin-3 (Bortmann et al., 1991) and sarafotoxin-S6b (Aumelas et al., 1991; Mills et al., 1991). Although the global conformation of this family of peptides is similar, some differences in the details of the secondary structural elements have been observed depending on the solvent conditions of the NMR experiments. In the various published structures, the length of the helix among family members has varied as well as the observance of a β-turn (residues 5–8).

To date only one other structure of big ET-1 has been reported (Inooka et al., 1991). Although the global fold of their structures is consistent with the structures presented here, it is difficult to compare the two studies since experimental details such as solvent conditions were not reported and their study was carried out at a much higher temperature (40°C) than our experiments (20°C). (The coordinates of the structures reported here will be submitted to the Brookhaven Protein Data Bank.)

ACKNOWLEDGEMENTS

We would like to thank Dr. S.C. Brown for helpful discussions and critical reading of this manuscript and Dr. J. Berman for providing us with unpublished results.

REFERENCES

Aumelas, A., Chiche, L., Mahe, E. and Le-Nguyen, D. (1991) *Neurochem. Int.*, **18**, 471–475.
Bax, A. and Davis, D. (1985) *J. Magn. Reson.*, **65**, 355–360.
Bek, E. and Berry, R. (1990) *Biochemistry*, **29**, 178–183.
Bortmann, P., Hoflack, J., Pelton, J. and Saudek, V. (1991) *Neurochem. Int.*, **18**, 491–496.
Brakch, N., Bousetta, H., Rholam, M. and Cohen, P. (1989) *J. Biol. Chem.*, **264**, 15912–15916.
Braunschweiler, L. and Ernst, R.R. (1983) *J. Magn. Reson.*, **53**, 521–528.
Brown, F.K., Hempel, J. and Jeffs, P.W. (1992) *Proteins* **13**, 306–326.
Crippen, G. (1977) *J. Comp. Phys.*, **24**, 96–107.
Crippen, G. (1981) *Distance Geometry and Conformational Calculations*, Research Studies Press, Wiley, Chichester.
Donlan, M., Brown, S. and Jeffs, P. (1991) *J. Cell. Biochem.*, **S15G**, 85.

Emori, T., Hirata, Y., Ahta, K., Shichiri, M., Shimokado, K. and Marumo, F. (1989) *Biochem. Biophys. Res. Commun.*, **162**, 217–233.

Fesik, S., Holleman, W. and Perun, T. (1987) *J. Magn. Reson.*, **74**, 366–371.

Havel, T., Crippen, G., Kuntz, I.D. and Blaney, J. (1983) *J. Theor. Biol.*, **104**, 383–400.

Hempel, J. (1989) *J. Am. Chem. Soc.*, **111**, 494–495.

Hyberts, S.G., Marki, W. and Wagner, G. (1987) *Eur. J. Biochem.*, **164**, 625–635.

Ikegawa, R., Matsumara, U., Tsukahara, Y., Takaoka, M. and Morimoto, S. (1990) *Biochem. Biophys. Res. Commun.*, **171**, 669–675.

Inooka, H., Endo, S., Kikuchi, T., Wakimasu, M., Mizuta, E. and Fujino, M. (1991) *Peptide Chemistry*, **28**, 409–414.

Inoue, A., Yanagisawa, M., Takuwa, Y., Kobayashi, M. and Masaki, T. (1989) *Proc. Natl. Acad. Sci. U.S.A.*, **86**, 2863–2867.

Jeener, J., Meier, B.H., Bachmann, P. and Ernst, R.R. (1979) *J. Chem. Phys.*, **71**, 4546–4553.

Kimura, S., Kasuya, Y., Sawamura, T., Shinmi, O., Sugita, Y., Yanagisawa, M., Goto, K. and Masaki, T. (1988) *Biochem. Biophys. Res. Commun.*, **156**, 1182–1186.

Kimura, S., Kasuya, Y., Sawamura, T., Shinmi, O., Sugita, Y., Yanagisawa, M., Goto, K. and Masaki, T. (1989) *J. Cardiovasc. Pharmacol.*, **13**, S5–S7.

Kloog, Y. and Sokolovsky, M. (1989) *Trends Pharmacol. Sci.*, **10**, 212–214.

Kraulis, P.J., Clore, G.M., Nilges, M., Jones, T.A., Petterson, G., Knowles, J. and Gronenborn, A.M. (1989) *Biochemistry*, **28**, 7241–7257.

Krystek, S., Bassolino, D., Novotny, J., Chen, C., Marschner, T. and Anderson, N. (1991) *FEBS Lett.*, **281**, 212–218.

Matsumara, Y., Hisaki, K., Takoaka, M. and Morimoto, S. (1990) *Eur. J. Pharmacol.*, **185**, 103–106.

Mills, R., Atkins, A., Harvey, T., Junius, K., Smith, R. and King, G. (1991) *FEBS Lett.*, **282**, 247–252.

Mueller, L. (1987) *J. Magn. Reson.*, **72**, 191–196.

Munro, S., Craik, D., McConville, C., Hall, J., Searle, M., Bicknell, W., Scanlon, D. and Chandler, C. (1991) *FEBS Lett.*, **278**, 9–13.

Nerdal, W., Hare, D. and Reid, B. (1988) *J. Mol. Biol.*, **201**, 717–739.

Nerdal, W., Hare, D. and Reid, B. (1989) *Biochemistry*, **28**, 10008–10021.

Nichols, J., Wiseman, J., Hassman, F., Rimele, T., Queen, K. and Berman, J. (1990) *FASEB. J.*, **4**, A959.

Okada, K., Takada, J., Arai, Y., Matsuyama, K. and Yano, M. (1991) *Biochem. Biophys. Res. Commun.*, **180**, 1019–1023.

Ohnaka, K., Takayanagi, R , Yamauchi, T., Okazaki, H., Ohashi, M., Umeda, F. and Nawata, H. (1990) *Biochem. Biophys. Res. Commun.*, **168**, 1128–1136.

Olejniczak, E., Gampe, R., Rockway, T. and Fesik, S. (1988) *Biochemistry*, **27**, 7124–7131.

Pollack, D. and Opgenorth, T.J. (1991) *Am. J. Physiol.*, **261**, R257–R263.

Rance, M., Sorensen, O.W., Bodenhausen, G., Wagner, G., Ernst, R.R. and Wüthrich, K. (1983) *Biochem. Biophys. Res. Commun.*, **117**, 479–485.

Reilly, M. and Dunbar, J. (1991) *Biochem. Biophys. Res. Commun.*, **178**, 570–577.

Rholam, M., Nicolas, P. and Cohen, P. (1986) *FEBS Lett.*, **207**, 1–5.

Saida, K., Mitsui, Y. and Ishida, N. (1989) *J. Biol. Chem.*, **264**, 14613–14616.

Sawamura, T., Kimura, S., Shinmi, O., Sugita, Y., Yanagisawa, M. and Masaki, T. (1989) *Biochem. Biophys. Res. Commun.*, **162**, 1287–1294.

Simonson, M.S. and Dunn, M.J. (1991) *Hypertension*, **17**, 856–863.

Singh, U.C., Weiner, P.K., Caldwell, J. and Kollman, P.A. (1986) *AMBER 3.0 USCF.*

Summers, M., South, T., Kim, B. and Hare, D. (1990) *Biochemistry*, **29**, 329–340.

Theriault, Y., Boulanger, Y., Weber, P. and Reid, B. (1987) *Biopolymers*, **26**, 1075–1086.

Watanabe, T., Itahara, Y., Nakajima, K., Kumagaye, S., Kimura, T. and Sakakibara, S. (1991) *J. Cardiovasc. Pharmacol.*, **17**, S5–S9.

Weber, P., Morrison, R. and Hare, D. (1988) *J. Mol. Biol.*, **204**, 483–487.

Weiner, S.J., Kollman, P., Case, D., Singh, C., Ghio, C., Alagona, G., Profeta, S. and Weiner, P. (1984) *J. Am. Chem. Soc.*, **106**, 765–784.

Wüthrich, K. (1986) *NMR of Proteins and Nucleic Acids*, Wiley-Interscience, New York, NY.

Yanagisawa, M., Kurihara, H., Kumura, S., Tomobe, Y., Kobayashi, M., Mitsui, Y., Goto, K. and Masaki, T. (1988) *Nature*, **332**, 411–415.

Yanagisawa, M. and Masaki, T. (1989) *Trends Pharmacol. Sci.*, **10**, 374–378.